Progress on X-ray computed tomography (CT) scanning in permafrost studies

F. Calmels, W. R. Clavano, & D.G. Froese
Department of Earth and Atmospheric Sciences – University of Alberta, Edmonton, Alberta, Canada.

ABSTRACT

Computed tomography (CT) scanning is used increasingly in engineering and earth science studies, but has been developed essentially for medical applications, thus there is a lack of data processing and analytical tools for geoscience studies. We present a simple method to digitally process CT scan images of permafrost cores. A Matlab script was developed which allows volumetric contents of gas, ice, and other inclusions to be determined. In addition to classical cryostratigraphical differences between sediment, ice and gas, CT scanning is used to characterize the cryotexture of cores by using volumetric contents. We demonstrate our methodology using natural permafrost samples from the Klondike area, central Yukon.

RÉSUMÉ

La tomodensitométrie (TDM) est utilisée de plus en plus en géosciences et en ingénierie, mais la technique fut développée pour un usage médical, aussi il existe un manque d'outils dédiés aux traitement et analyse des données issues des études du pergélisol et des géosciences. Les auteurs présentent ici une méthode simple de traitement digital des images scanographiques d'échantillon de pergélisol. Un script Matlab permettant la détermination des contenus volumétriques en glace, gaz et autres inclusions a été développé.   En plus des distinctions cryostratigraphiques classiques entre sédiment, glace et gaz, la scanographie est utilisée pour caractériser la cryostructure des échantillons en utilisant les contenus volumétriques sous forme de spectrogrammes de densité. Des échantillons naturels de pergélisol de la région du Klondike, Yukon central, servent à démontrer notre méthodologie.

1   INTRODUCTION

Over the last decade, computed tomography (CT) has seen increased utility in the earth and engineering sciences (Mees et al., 2003). CT scanners are now found in many non-medical scientific research institutions. While the instruments continue to be developed and the techniques for analysing the resulting images evolve, the analytical tools remain mostly medically-oriented (e.g., ImageJ by the NIH, Rasband, 1997-2009).   Beyond simple imaging and algorithms for analysis, there is a lack of programs available that are dedicated to treatment of data from the earth sciences, in particular to permafrost scans.

The current note presents progress in using CT scans for permafrost cores, along with an algorithm to process the resulting images that allows for the determination of the volume fraction of gas, ice, and sediment in natural permafrost samples. Validation of the volumetric content calculations are made by analyzing a synthetic sample fabricated from a collection of large pebbles, immersed in water to make up a known volume and subsequently frozen.

2   CT SCAN AND PERMAFROST STUDIES

CT scanning has proven to be highly useful for permafrost studies (e.g., Calmels and Allard 2004, 2008). Because it is a non-destructive technique, the permafrost cores remain available for further sedimentological, geotechnical, and geochemical   analyses. At the same time, the three-dimensional images provide an objective quantification of material properties as well as structural characteristics that will inform further sub-sampling and

contribute comparative information to other more traditional procedures.

The resolution of the permafrost images depends on the X-ray instrument used for scanning. On average, one can expect to interpret images at the millimetre scale, which is appropriate for observing ice lenses and individual gas bubbles. The orientation of the entrained ice and gas during freezing and refreezing can be used to establish the processes that took place during permafrost evolution. Diagenetic changes such as water migration, gas segregation into bubbles and cavities, and volume change that may be related to deformation can be inferred. In previous studies (Calmels and Allard 2004, 2008), medical software that was used for analysis was limited to visualization using user-defined density cutoff values and volumetric content determination using only two orthogonal longitudinal image. It became apparent that a better method needed to be developed to effectively utilize all the information that was available. In this paper we present recent progress with a simple approach that would take into account every single slice of the set of scans forming a section of a permafrost core.

3   VOLUMETRIC   CALCULATION   PROCEDURE USING MATLAB

3.1 Samples

Natural permafrost samples were collected from the Klondike region in the Yukon. These were taken close to the surface (up to a depth of about 3m) and are described in Calmels and Froese (2009) and Calmels et al. (in review). CT scanning is a non-destructive radiographic approach to examine materials in their natural state

creating a three-dimensional map of density contrasts. Density measurements are made relative to water and expressed in Hounsfield Units (HU). Water thus has a value of 0HU and air about -1000HU. The resulting images are usually represented in greyscale so that darker tones (more black) indicate lower density material and lighter tones (more white) higher density. By scanning a core from top to bottom (or vice versa), a three-dimensional "stack" of images (not shown) is produced by compiling individual (transverse) "slices" (Figure 1). Extracting longitudinal sections across slices produces a "profile" of the core section (Figure 2). Imaging was accomplished using a Toshiba Aquilion 64 X-ray scanner, owned and operated by the Alberta Research Council in Edmonton, which can achieve a spatial resolution of 0.35mm in the transverse direction and 0.5mm in the longitudinal direction.
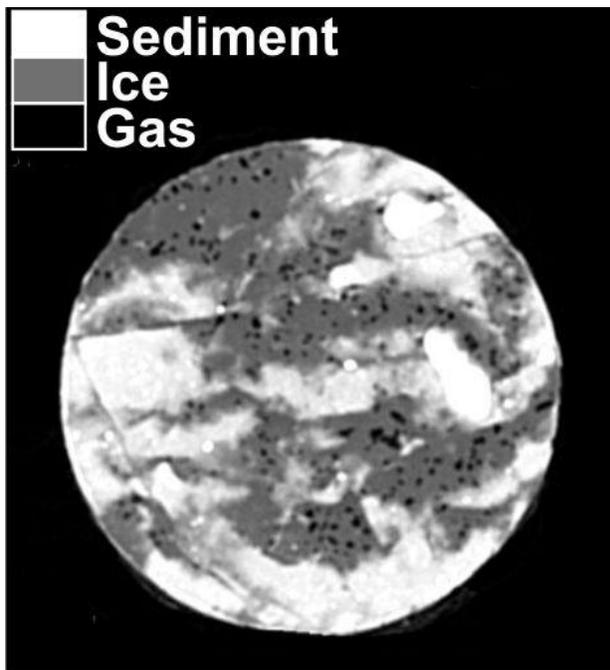

Figure 1. Transverse slice.
Sediment is white, ice is grey and gas is black.

3.2 Using histograms to determine image classification criteria

In general, cryostructural studies focus on the three main permafrost components: sediment (inorganic and organic), ice, and gas. By creating a histogram of values from each sample, a distribution of density values (in HU) is presented (Figure 3). The shape of the histogram changes with the proportion of the component materials. In fact, a histogram is a representation of the volumetric content in a sample.

The frequency counts are made from a complete set of CT scan images, representing a single sample. A maximum of 100 cm of core is imaged at one time, using the maximum resolution of the instrument (0.35 mm). Such sections contain about 2,800 slices (e.g., about 1.39 Go of information), which can still be easily digitally

processed. Figure 3 shows a histogram of a section that is mostly of high-density material with some ice (intensity values along the x-axis and normalized frequency counts along the y-axis). The raw count is shown in grey as a bar plot. Notice that there is a peak around 0HU, which is the value for water. For ice, we can expect values in the range -150 to -40HU. It seems that we have material in the core with densities very close to water/ice, however, a cutoff point is apparent from the histogram: it would be the lowest frequency count between the two peak values.
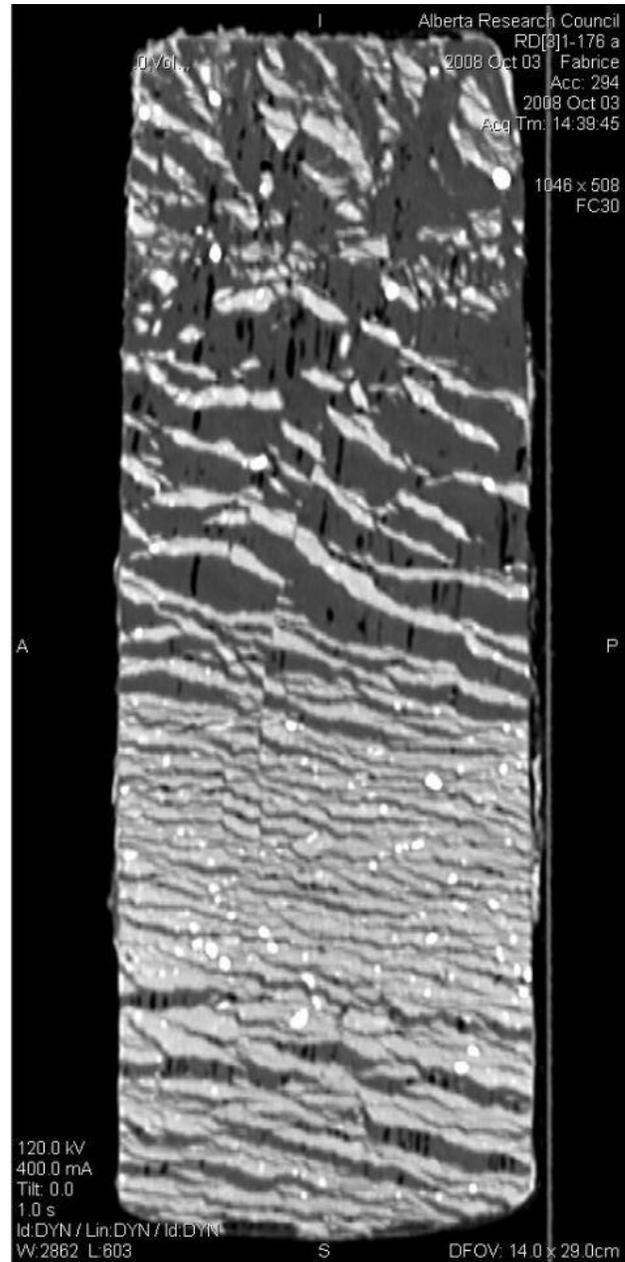

Figure 2. Longitudinal section.
Sediment is white, ice is grey and gas is black.
This is a profile of the sample shown in Figure 1.

It is not always the case that the lowest point is close to the limit of the density value for water/ice, so this cutoff needs to be properly selected. Furthermore, we developed a Matlab function to fit multiple Gaussian functions to help automate the selection of a cutoff value (blue vertical line in Figure 3), as well as to determine peak values (blue asterisks in Figure 3). We assume that the values are normally distributed. It is not important at this point that the fitted curve (red in Fig. 3) matches the histogram as closely as possible; it is only a guide for determining an appropriate cutoff value. The Matlab fitting function is described in a subsequent paper (Clavano et al, in prep.), and can fit any number (up to eight) of Gaussian curves to an empirical histogram.
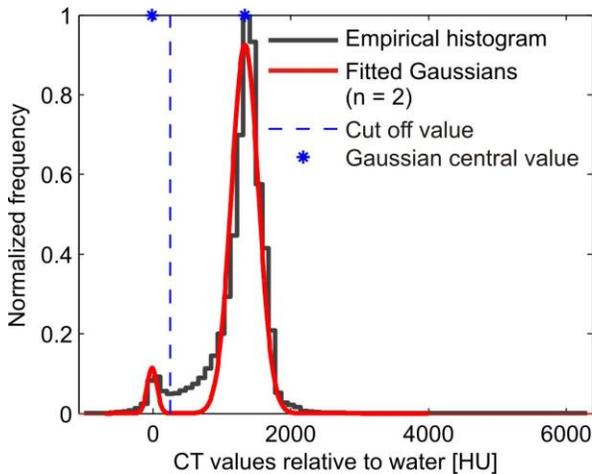

Figure 3. Empirical and fitted histograms with two density peaks.

A histogram with four (possibly more) peaks is shown in Figure 4. This time the histogram is characteristic of a gas-rich core, with abundant bubbles. There is also some amount of ice and a distribution of sediment, which could be of two main types, as indicated by the two different density peaks. The cutoff values are chosen by examining the parameters of the fitted curves (i.e., standard deviations). It is possible that the fitting procedure does not result in an appropriate fit. In this case, a manual selection of cutoff values is necessary, done by examining the peaks and troughs of the histogram.

It is not always the case, however, that the density peaks are distinguishable from one another. By increasing the number of bins in the histogram, it is possible to find the first (ice) peak (Figure 5). When this happens, it will be the usual case of having difficulty in telling water/ice and lower density material apart. But we know the possible range of values for water/ice, so that even when increasing the number of bins in the histogram does not uncover an ice peak, the Gaussian fitting process will help to determine the central (peak) value of the ice distribution thereby producing a usable cutoff value (Figure 6).
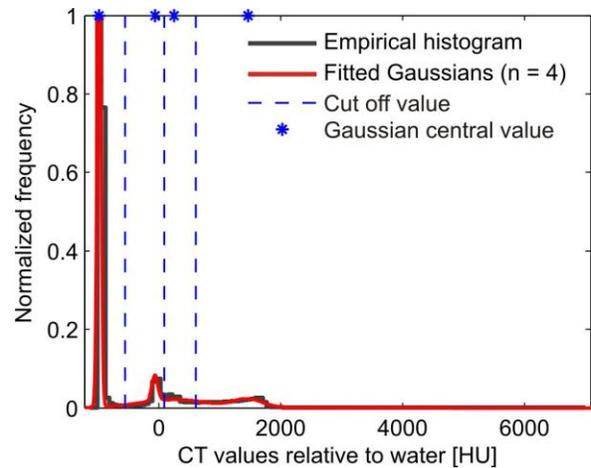

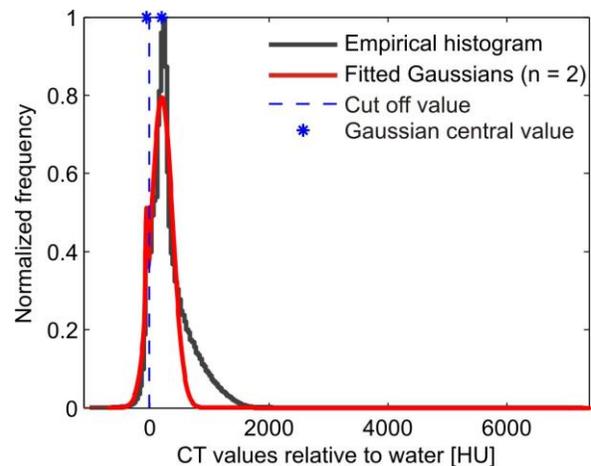Figure 4. Empirical and fitted histograms showing four density peaks.

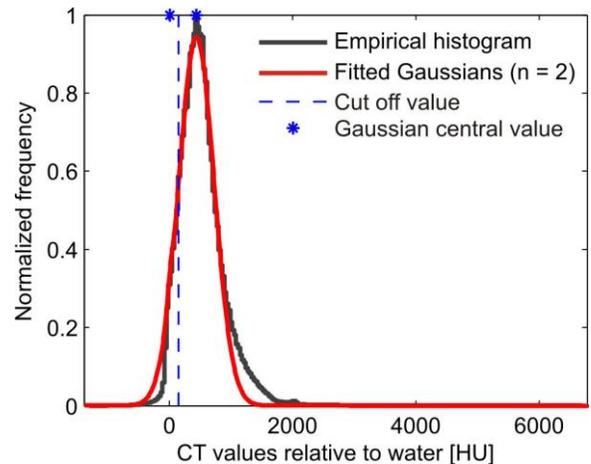Figure 5. Empirical and fitted histograms with increased bins in the histogram.

Figure 6. Empirical and fitted histograms with two density peaks.

3.3 Setting the core boundary

Before we can proceed to determine volume fractions for gas, ice, and sediment, we need to determine which pixels in each slice image belong to the core section and which do not (e.g., sample container, accreted dirt along the core wall, the supporting bench, and surrounding air). This can be done by manually examining each individual slice and drawing a boundary around it to select only the pixels of interest. However, with about thousands of slices in each sample, we would like to automate the procedure to speed up the analyses. For a perfectly circular transverse slice, using the cutoff value for air (around -150HU) will serve as a boundary. It happens that sometimes air bubbles/pockets can occur close to the wall. In this case, we need to find a way to bound the slice to include these legitimate bubbles. We do this by finding a convex hull that wraps around the initial air-based boundary. When this new boundary is much larger than the initial one, as is the case at the top and bottom slices of a section, we disregard the slice. This is just a simple way of excluding ambiguous sections that are already likely contaminated during transit and storage without disregarding portions of the core that might still hold important information.

3.4 Volume fractions

Once the boundaries of each core slice have been defined, we determine the number of pixels with values falling within the HU ranges for gas, ice, and sediment. Figure 7a shows an example of a core boundary delineation (red line), with the core HU values shown in greyscale. A count of how many image pixels fall within that boundary constitutes the total volume of material for this slice. Using the histogram cutoff values again allows a classification of pixels into gas, ice, sediment, simplifying the visualization; see Figure 7b. The darkest pixels are air bubbles/pockets, dark grey represents ice (bounded by blue), and the lighter tones are sediment. By counting how many pixels are classified as gas, ice, or sediment, we can determine its fraction to the total volume of material. Air and ice in this example constitutes almost one-third of the total volume.

To test and validate our calculation procedure, synthetic samples, with known sediment, water, and total volumes, were scanned and analysed. The samples, ranging from very coarse sand to medium gravel, were saturated with water and then frozen. Water volume expansion due to freezing was assessed, and the uncertainties for each element were deduced from the Matlab volume calculations. Results suggested that when a pixel was identified, the calculation was wrong only 2-4% of the time for ice, 1-7% for the sediment, and about 1% for gas (Clavano et al., in preparation). These uncertainties provide a baseline for the calculations, as synthetic samples only contained pore ice. Uncertainties should decrease with increasing excess ice content. The uncertainties relate mostly to instrumental limitations.
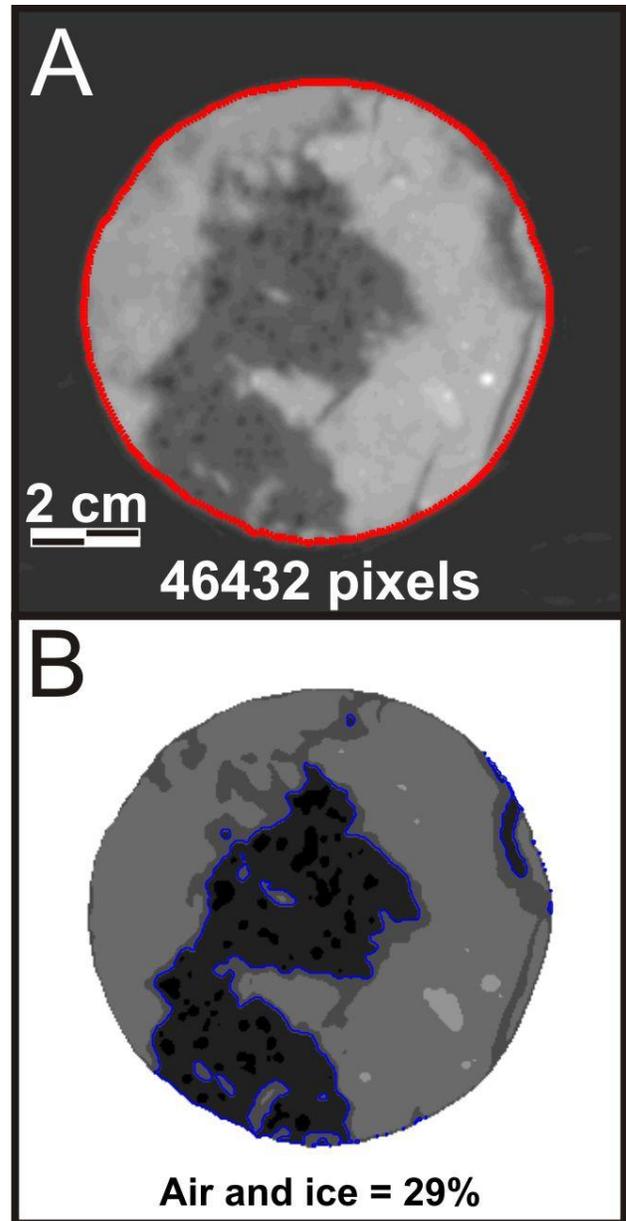

Figure 7. Volume calculation procedure. A- boundary definition on a grey scale image, B- volume calculation using a classified image.

4   LIMITATIONS

Using electromagnetic radiation to image physical properties of permafrost material makes CT scanning an indirect method and makes useful the application of remote sensing techniques.   The X-ray images are produced by exploiting the density contrast in the material, with the image resolution dependent on the instrument used.   The scanning method is relatively accurate, but it is not free from error. Most of these errors are known and can be corrected by image processing. Nevertheless, for our purposes, two main limitations remain: material densities close to the density of water are difficult to distinguish from water/ice, and materials that have sizes smaller than the resolution of the instrument can be incorrectly classified.

When two different materials sharing very similar densities exist (one of these is usually ice), an investigator needs to know in advance when this is the case. This can happen, for example, when organic-rich horizons occur. Material such as peat embedded in permafrost can have densities very similar to ice. This can happen because peat is usually entrained in ice and that the ice densities dominate the signal. A volume correction factor is possible if the volume of peat could be determined by other methods post-scan. This issue, however, could also be considered as an instrumental resolution problem. For example, if we had material such as peat, but with very different densities from ice, its size would still be smaller than the resolution of the instrument. Its density will be drowned out by the surrounding ice and will likely show up as a "mixed" pixel with densities perhaps a little higher than ice but will not be correctly classified.

A similar issue related to the limitation of instrument resolution is the discrimination of pore ice from fine-grained sediment. For fine-grained material, a pixel resolution of 0.35mm will represent a composite density value created by the particular mix. In the same way, small particles (e.g., gas bubbles) with sizes smaller than 0.35mm and imbedded in ice cannot be accounted for in the calculation. Because of these limitations, accuracies for volumetric determinations are improved when dealing with material having low organic content and/or ice lenses thicker than 0.35 mm.   These uncertainties are further descussed in a subsequent paper (Clavano et al., in prep).

5   PROSPECTS AND CONCLUSION

Volumetric ice content is an important parameter that is used to determine ground settling induced by permafrost degradation. It can also provide information about cryogenetic processes and permafrost dynamics, as well as contribute to local permafrost history (e.g., Calmels and Froese 2009, Calmels et al., in review). Similarly, the CT scanning method can accurately provide volumetric gas content. There is a rising concern about the consequences of gas volume discharge that would follow permafrost melting in the next few decades. A goal of the Matlab script is to provide a tool to better quantify the gas and ice components in permafrost samples. It is intended to be an alternative (or complementary) and faster, procedure than traditional analyses. Laboratory analyses usually only provide mass content and involve destroying the samples, losing any information on structure.

The density occurrences are sample-specific, i.e., histogram shapes will vary between samples. However, we present a program that takes this into account and allow for a semi- or a completely automated image classification procedure. A cryofacies classification such as that defined by Murton and French (1988) that includes pure ice, sediment-poor ice, sediment-rich ice, ice-rich sediment, and ice-poor sediment, can be readily derived from the results of the procedure that we present here.   Some sedimentary properties can be assessed from the histogram, as expected, by pre-determining fine-grained, coarse-grained, and organic-rich sediments along a profile. Associating cryofacies to sedimentary properties will be the primary contribution of using CT scanning to classify permafrost samples. We intend to develop user-friendly programs from the scripts and distribute it freely to the community.

REFERENCES

Calmels, F. and Allard, M. 2004. Ice segregation and gas distribution in permafrost using tomodensitometry analysis. Permafrost and Periglacial Processes, 15: 367-378.

Calmels, F. and Allard, M., 2008. A structural interpretation of the palsa/lithalsa growth mechanism through the use of CT scanning. Earth Surface Processes and Landforms, 33: 209-225.

Calmels, F. and Froese, D.G. 2009. Cryostratigraphic record of permafrost degradation and recovery following historic surface disturbances, Klondike area, Yukon. Yukon Exploration and Geology 2008: 85-97.

Calmels, F., Delisle G. and Allard, M. 2008. Internal structure and the thermal and hydrological regime of a typical lithalsa: significance for permafrost growth and decay. Canadian Journal of Earth Sciences, 45: 31-43

Calmels, F. Froese, D.G. and Clavano, W. In review. Testing permafrost resilience using historical disturbances in the Klondike area, Yukon, and recovery of ancient permafrost cores. Canadian Journal of Earth Sciences.

Mees, F., Swennen, R., Van Geet, M. and Jacobs, P. 2003. Applications of X-ray Computed Tomography in the Geosciences. Geological Society, London, Special Publications, UK.

Murton J. B. and French H. M. 1994. Cryostructures in Permafrost, Tuktoyaktuk Coastland, western Arctic Canada. Canadian Journal of Earth Sciences, 31: 737-747.

Rasband, W.S., ImageJ, U. S. National Institutes of Health, Bethesda, Maryland, USA, http://rsb.info.nih.gov/ij/, 1997-2009.